

Coupled Electric/Thermal/Fluid Analysis of High Voltage Bushing

Göran Eriksson*¹

¹ABB AB, Corporate Research

*Corresponding author: SE-721 78, Västerås, Sweden, goran.z.eriksson@se.abb.com

Abstract: Modern power transmission systems often operate at high voltage and current levels, which introduce challenges when it comes to electrical insulation and cooling issues. In this paper we illustrate a COMSOL Multiphysics model that solves for the strongly coupled set of equations describing the distribution of the electric field, the temperature, and the flow of a cooling liquid in a high voltage bushing.

Keywords: High voltage bushing, Electric field, Temperature, Fluid flow, Coupled equations.

1. Introduction

Modern power transmission systems are in general designed to operate at high voltages in order to reduce resistive losses generated by high currents. This, however, tends to increase the risk for dielectric breakdown or flashovers if the equipment is not properly designed to withstand the stress. Out of the many components comprising the transmission system some of the most stressed are the so-called bushings, i.e. feed-through devices preventing flashover between a grounded conducting wall and a high voltage conductor penetrating the wall. Such bushings can for instance be used to connect transformer windings to high voltage feeding cables outside the oil-filled transformer tank, see Fig. 1. Other applications involve smaller power devices placed inside oil-filled containers or high voltage conductors connecting the different valve and reactor halls in an HVDC converter station. The present work illustrates the necessity of using strongly coupled multiphysics simulations in order to properly describe and understand the complex behavior of a high voltage bushing.

2. DC bushing

Here we consider a rather unconventional design of a bushing for feeding a DC current at high voltage through a grounded conducting container wall. Contrary to the transformer AC bushings seen in Fig. 1 it penetrates the bottom of the container.



Figure 1. A large power transformer having long high voltage and smaller low voltage bushings mounted on top of the oil-filled transformer tank.

The outside of the grounded container is surrounded by air while on the inside the container is filled with mineral oil acting both as an electrical insulator and a cooling liquid. For the sake of mounting flexibility the bushing partly consists of a modified version of a standard ABB cable termination. A layer of a so-called field grading material (FGM) ensures that the field stress is distributed relatively smoothly. The axisymmetric geometry of the DC bushing is shown in Fig. 2.

2. Electric and thermal stress

The problem basically consists of minimizing the size and cost of the bushing while keeping the internal electric stress levels and the temperature rise within acceptable limits.

Since we are studying a DC bushing the leakage current, and hence the electric field distribution, is to a large extent determined by the very small electric conductivities of the different insulating materials inside the bushing. These conductivities are in turn dependent on the local temperature. In addition, the FGM material has a strongly E-field dependent conductivity.

The heat balance equation, with the resistive heating as source term, thus becomes strongly coupled to the equation governing the electric field, or current, distribution.

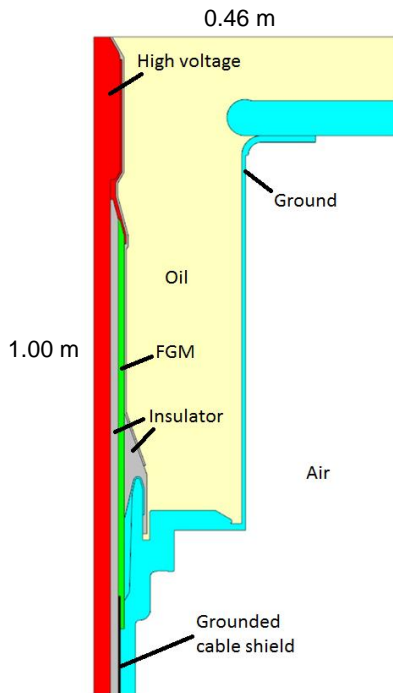


Figure 2. Axisymmetric model of a DC bushing penetrating the bottom of the container.

Moreover, most of the heat transported away from the solid inner parts of the bushing is removed via natural convection in the oil and then transferred to the surrounding air. It is therefore crucial to solve for the oil flow pattern as well, a task which is further complicated by the fact that the viscosity is highly temperature dependent.

From the above discussion it is clear that we are facing a strongly coupled multiphysics problem involving strong nonlinearities. In order to solve for the electric field, temperature, and oil flow velocity a numerical simulation is required.

3. Model equations

The model has been implemented in several of the earlier versions of COMSOL Multiphysics but the information given below refers to the latest version, 4.3.

3.1 Heating of high voltage inner conductor

The high voltage inner conductor influences the problem in two different ways. First, it provides

one electrode for the electric field and leakage current between the inner conductor and the grounded housing. This is described in Section 3.4. Second, it serves as the main heat source in the system because of the resistive heating generated by the high current (of the order of 1 kA) through the conductor. This current is several orders of magnitude larger than the leakage current through the imperfect insulators, which in turn allows us to only consider the inner conductor domain when calculating the current distribution, and hence the resistive heating, inside it. The equations solved by the stationary *Electric Currents* interface are:

$$\begin{aligned}\nabla \cdot \mathbf{J} &= Q_j \\ \mathbf{J} &= \sigma \mathbf{E} + \mathbf{J}_e \\ \mathbf{E} &= -\nabla V\end{aligned}\quad (1)$$

where $Q_j = 0$ and $\mathbf{J}_e = 0$ in our case. Boundary conditions are: *Electric Insulation* on the cylindrical surface, *Ground* on one end surface, and *Floating Potential* prescribing the total current through the other end surface. It is here important to note that it is crucial to include the temperature dependence of the copper conductor conductivity.

3.2 Heat transport

The next equation to consider is the heat balance, or heat transport, equation for the temperature T :

$$\rho C_p \mathbf{u} \cdot \nabla T = \nabla \cdot (k \nabla T) + Q \quad (2)$$

Here, ρ , C_p , and k are the density, specific heat, and heat conductivity, respectively. Convective heat transport is described by the term containing \mathbf{u} , the fluid flow velocity (nonzero only in the oil domain). Q is the heat source distribution, which mainly consists of the resistive heating generated in the inner high voltage conductor, see Section 3.1, but also has a small contribution from the leakage current flowing through the imperfect insulators. Equation (2) is solved using the *Heat Transfer in Fluids* interface applied in all material domains. Appropriate boundary conditions are applied on external surfaces and have a significant influence on the solution. For instance cooling to the surrounding air volume at ambient temperature is described by a heat transfer coefficient.

3.3 Fluid flow

Most of the heat generated is removed via convection and heat conduction in the oil volume, as described by (2). It turns out that convection is the by far most important mechanism. Consequently, a reasonably accurate solution for the flow velocity \mathbf{u} is required. This is provided by the *Laminar Flow* interface, where the equations for incompressible laminar flow are being solved:

$$\begin{aligned} \rho(\mathbf{u} \cdot \nabla)\mathbf{u} = \\ \nabla \cdot \left[-p\mathbf{I} + \mu(\nabla\mathbf{u} + (\nabla\mathbf{u})^T) \right] + \mathbf{F} \quad (3) \\ \rho \nabla \cdot \mathbf{u} = 0 \end{aligned}$$

Here, the unknowns are \mathbf{u} and the pressure p . The viscosity μ has a strong temperature dependence and we assume an analytical relationship of the form $\mu = \mu_0 \exp(-T/T_0)$. Finally, \mathbf{F} is the vertical buoyancy force caused by a temperature gradient in the fluid. This force is proportional to the difference between the local temperature and a constant average temperature.

Boundary conditions are no-slip (i.e. $\mathbf{u} = 0$) on all boundaries except the top interface connecting to a much larger oil-filled volume. Here, we apply the *Open Boundary* condition.

It should be mentioned that in many realistic cases the viscosity of the fluid becomes so low that convergence is difficult to achieve. Various tricks, such as variation of parameters and/or relaxed convergence criteria, may help.

3.4 Electric field and current distribution

The last set of equations needed are those governing the overall electric field and current distribution outside the inner high voltage conductor. To do this we introduce a second *Electric Currents* interface node, independent from that of Section 3.1. The same set of equations (1) are solved but this new node is active everywhere except inside the inner conductor. Boundary conditions are simple, viz. *Ground* on the conducting housing and a high voltage *Electric Potential* (of the order of 100 kV) on the surface of the inner conductor. The nonlinearity of the problem is increased by the fact that the "insulating" materials have electric

conductivities that are dependent on both the temperature and the local electric field. These dependences are described using exponential functions. In particular the conductivity of the FGM material varies extremely strongly with the electric field. This provides the desired stress-smoothing property of such materials.

4. Results

The coupled system of equations is solved in a single run using a triangular mesh with 49 503 elements, resulting in 233 511 unknowns. The solution time is about 5 minutes on an HP Elite Book laptop equipped with an Intel® Core™ i7-740QM CPU at 1.73 GHz.

Simulations are performed assuming that the inner conductor carries a current of 2 kA and is at a voltage of 80 kV. The ambient air temperature is taken to be 20 °C.

Figure 3 shows the distribution of resistive heating power in the inner copper conductor. As can be seen the heating is strongly dependent on the local radius of the conductor, or equivalently the current density.

Next, the temperature distribution is displayed in a 3D representation in Fig. 4. In the 2D plot (5) there is also shown the total heat flow in the oil and the conductive heat flow in the solid parts.

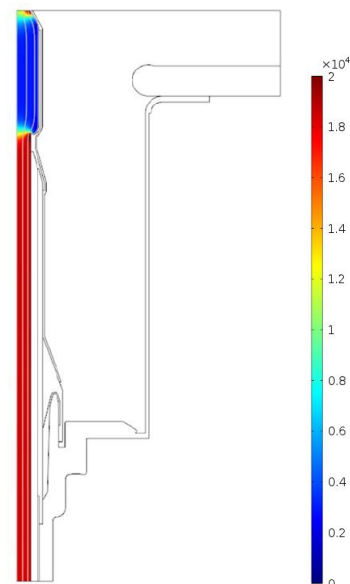


Figure 3. Resistive heating power density (W/m^3) in the current-carrying inner conductor.

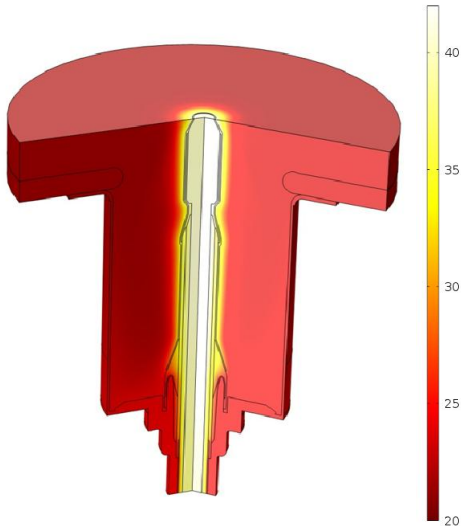


Figure 4. 3D representation of the temperature distribution.

Note that the amount of heat transported away by oil convection into the very large oil volume above the computational domain is substantial.

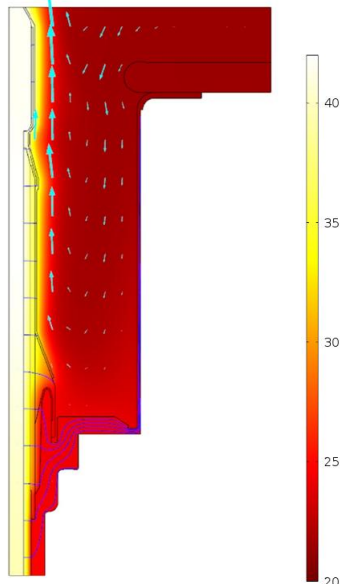


Figure 5. 2D representation of the temperature distribution. Light blue arrows indicate the total heat flow in the oil while dark blue streamlines denote the conductive heat flow in solid parts.

We also see that the insulator material parts closest to the inner conductor are not subjected to temperatures higher than 42 °C, which is acceptable.

An important mechanism for removing heat from the system is obviously convection due to the self-circulating oil flow. This quantity is shown in Fig. 6, where the flow pattern is displayed as white streamlines and the velocity amplitude corresponds to the color code. We immediately observe the large upward flow close to the hot inner conductor.

Finally, we examine the critical issue of the electric field stress level inside the bushing. Highest stress levels can in Fig. 7 be seen close to sharp edges at ground and high potential, as well as in the cable insulation layer between the inner conductor and the FGM adapter. These levels are, however, in this case acceptable. Note the equidistant distribution of equipotential curves in the FGM material, resulting in a smooth electric field distribution.

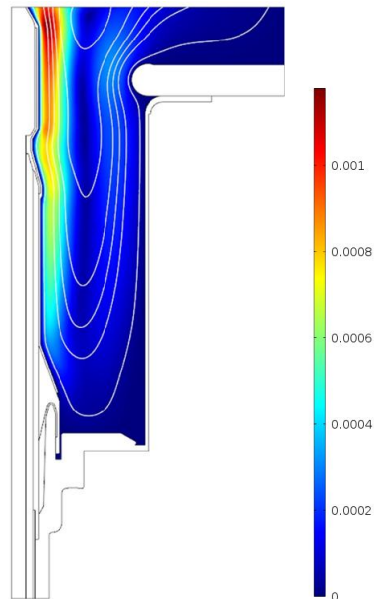


Figure 6. Oil flow pattern. White curves show flow streamlines and surface color denotes flow velocity amplitude.

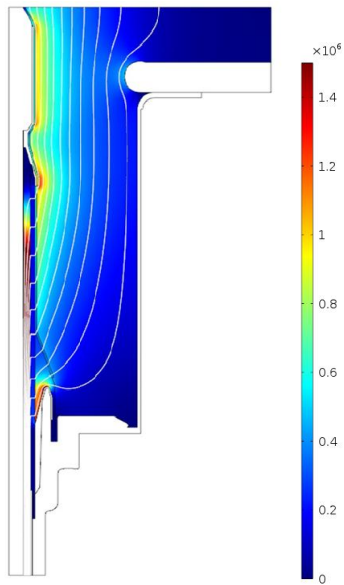


Figure 7. Electric field distribution. Equipotential curves are shown in white while surface color denotes electric field amplitude

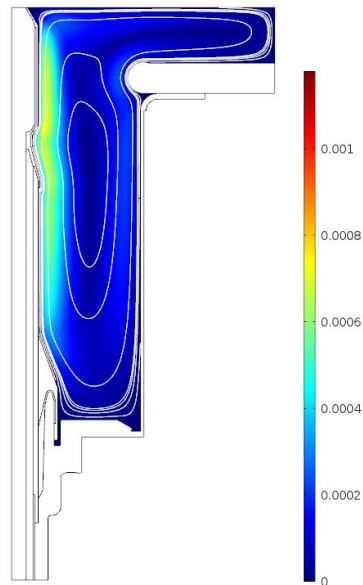


Figure 8. Velocity distribution. Same as Fig. 6 but now with no heat and oil flow across the upper boundary of the oil domain.

5. Importance of convection cooling

The importance of describing the oil flow sufficiently accurately can be demonstrated by two examples; (i) one where no heat or oil can flow across the upper boundary of the oil domain, and the other (ii) where the convective heat transport is not at all included in the heat balance equation (2), i.e. $\mathbf{u} = 0$ is assumed.

For case (i) we see from Fig. 8 that the velocity of the circulating oil is now significantly lower. The convective heat transport is thus smaller and consequently the cooling becomes worse, as is observed in the temperature plot Fig. 9. The maximum temperature is 44 °C.

In the second case, (ii), the flow velocity is set to zero everywhere, leading to a situation where the only way the oil can transport heat is via conduction. The temperature now reaches 54 °C.

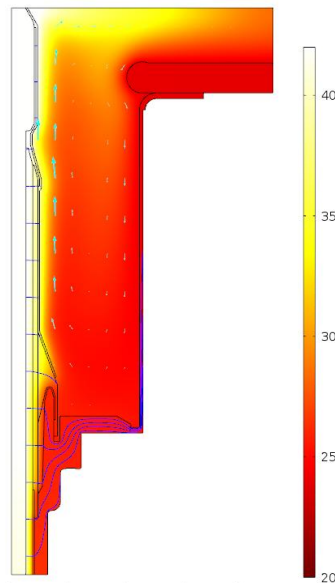


Figure 9. Temperature distribution. Same as Fig. 5 but now with no heat and oil flow across the upper boundary of the oil domain.

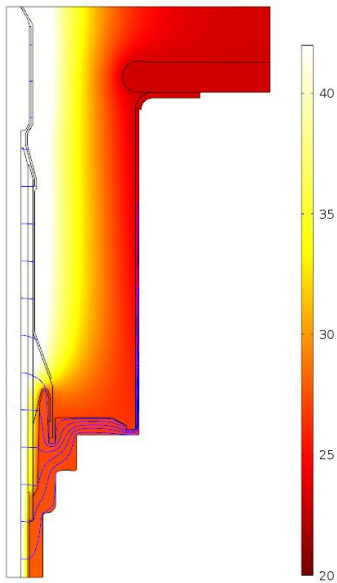


Figure 10. Temperature distribution. Same as Fig. 5 but now with zero flow velocity in the oil domain.

6. Conclusions

With increasing requirements for higher ratings in terms of voltage and transmitted power, electric and thermal stress issues become crucial for power transmission equipment. Some of the most severely stressed components are bushings. In this paper we have demonstrated the usefulness of multiphysics simulations in order to solve the complex system of equations describing the strongly coupled phenomena involved. This provides invaluable help not only in the design work but, occasionally, also for finding failure causes.

The simulations shown here have been purely stationary, corresponding to constant DC voltage and current. A similar approach can, however, also be applied to nonstationary transient stresses, for instance when switching or lightning pulses propagate along the cables connected to the inner conductor. The electric equations have to be solved in the transient mode but due to the short duration of such pulses compared to the typical time scales of the heat balance and fluid flow equations one can often use the stationary solutions of these. This simplifies the simulation considerably.